Antibody Screening Results for Anti-Nucleocapsid Antibodies Towards the Development of a SARS-CoV-2 Nucleocapsid Protein Analyte Detecting Lateral Flow Assay

David M. Cate[1*], Helen V. Hsieh[2], Veronika A. Glukhova[1], Joshua D. Bishop[1], Luis F. Alonzo[1], H. Gleda Hermansky[2], Brianda Barrios-Lopez[2], Ben D. Grant[1], Caitlin E. Anderson[1], Ethan Spencer[1], Samantha Kuhn[1], Ryan Gallagher[1], Rafael Rivera[1], Crissa Bennett[2], Samantha A. Byrnes[1], John T. Connelly[1], Puneet K. Dewan[1], David S. Boyle[3], Bernhard H. Weigl[1], Kevin P. Nichols[1]

1 - Global Health Labs, 14360 SE Eastgate Way, Bellevue, WA 98007
2 - Intellectual Ventures Laboratory, 14360 SE Eastgate Way, Bellevue, WA 98007
3 - PATH, 2201 Westlake Ave, Seattle, WA 98121

* Corresponding Author: David Cate – david.cate@ghlabs.org

Abstract

The global COVID-19 pandemic has created an urgent demand for large numbers of inexpensive, accurate, rapid, point-of-care diagnostic tests. Analyte-based assays are suitably inexpensive and can be rapidly mass-produced, but for sufficiently accurate performance they require highly optimized antibodies and assay conditions. We used an automated liquid handling system, customized to handle arrays of lateral flow immunoassay (LFA) tests in a high-throughput screen, to identify anti-nucleocapsid antibodies that will perform optimally in an LFA. We tested 1021 anti-nucleocapsid antibody pairs as LFA capture and detection reagents with the goal of highlighting pairs that have the greatest affinity for unique epitopes of the nucleocapsid protein of SARS-CoV-2 within the LFA format. In contrast to traditional antibody screening methods (e.g., ELISA, bio-layer interferometry), the method described here integrates real-time reaction kinetics with transport in, and immobilization directly onto, nitrocellulose. We have identified several candidate antibody pairs that are suitable for further development of an LFA for SARS-CoV-2.

Introduction

The emergence of the severe acute respiratory syndrome coronavirus 2 (SARS-CoV-2) has led to a global pandemic of COVID-19, infecting more than 81 million people worldwide in less than a year, and killing over 1.8 million persons by the end of 2020.[1,2] Strategies to suppress transmission of SARS-CoV-2, the virus that causes COVID-19, have been constrained by limitations in the availability of tests that can detect viral infection early. The predominant test format used to detect SARS-CoV-2 is reverse transcriptase polymerase chain reaction (RT-PCR), conducted most on specimens collected from the nasopharynx or oropharynx of symptomatic or exposed individuals. Demand for RT-PCR testing for SARS-CoV-2 in most of the world has exceeded the available supply.

Diagnostic testing is central to detecting the virus in symptomatic and asymptomatic persons, or those identified as contacts exposed to COVID-19 cases, to guide community interventions that are predicted to contain ongoing transmission. The pandemic has resulted in unprecedented demand for the RT-PCR testing capacity of all countries. Demand for testing has been coupled with a global shortage of commercial kits, reagents, consumables, disruptions in the global transport networks, and exacerbated

by international competition for testing resources. Accordingly, even many high-income countries have inadequate RT-PCR testing capacity to effectively suppress ongoing transmission, and most low and middle-income countries (LMICs) are unlikely to be able to establish even minimally needed RT-PCR capacity in the immediate future.

Direct analyte-based tests for SARS-CoV-2 offer an attractive alternative solution to testing needs and possibly the only viable solution for most LMICs. Analyte tests, which detect the presence of viral proteins, can be directly conducted on biological samples, such as tissue swabbed from the anterior nasal cavity, oropharynx, or even directly on saliva. Such analyte tests already exist for influenza, strep throat, and other infectious diseases. Analyte tests in the LFA test format already have extremely high production capacities in the billions of units/year, are inexpensive and easy to use, return results in minutes, and crucially, like RT-PCR and unlike serological tests, can reveal an active infection.

The use case for a low-cost, highly accessible SARS-CoV-2 test is strong even if the test were to be less sensitive than current RT-PCR testing. Modeling shows that decentralized, point-of-care testing with rapid return of results would have greater potential impact on transmission than the absolute limit-of-detection of the test.[3] These models build on the important observation that infectious viral particles have not been recovered below around 100 copies/mL.[4,5]

Rapid analyte tests are beginning to enter the commercial market. Thus far, however, few analyte tests for SARS-CoV-2, compared to nucleic acid tests, have received authorization from regulatory authorities worldwide. Therefore, a concerted effort is underway to catalyze the development of analyte-based rapid diagnostic tests that require no or minimal instrumentation, and to prepare manufacturing capability to meet the needs of the larger global market.[6] Required performance characteristics of a SARS-CoV-2 analyte detection assay have been published by the World Health Organization.[7]

A key step in the development of an LFA is the selection of selective antibodies for the target of interest. To expedite this process, our group has pioneered a high-throughput, robotic, antibody-screening process directly on nitrocellulose.[8] This method allows us to rapidly screen hundreds of combinations of antibodies more quickly than is typical of early-stage LFA development, while simultaneously utilizing nitrocellulose-specific reaction kinetics and flow rates that are difficult-to-impossible to mimic in other multiplexed analytical systems (e.g., ELISA, biolayer interferometry). Chemical gradients, residence times, binding orientations, affinity rates, drying and subsequent rehydration of reagents, and spatial distributions of antibodies are different in LFAs than in other immunoassays, and therefore, the best antibodies for LFAs may be different than for the best antibodies for ELISA, for example.

In this paper we describe the results of an extensive antibody screening effort that utilized our high-throughput, robotic, antibody-screening platform[8] to screen through 1021 unique combinations of antibodies that target the SARS-CoV-2 nucleocapsid protein. Over the course of several months, as various SARS-CoV-2-related reagents became available, five screening rounds were conducted against a total of three different sources of SARS-CoV-2 nucleocapsid analyte. We primarily focused on the outcomes of three screening rounds (one each against different recombinant analytes and one against a diluted positive clinical positive pool) to highlight the differences in antibody pair rankings we obtained as a function of analyte variant.

Materials and Methods

Reagents and materials

The following LFA reagents were purchased: Triton X-100, Tween 20, 10× PBS, sucrose, and IGEPAL CA-630 from Sigma Aldrich (St. Louis, MO, USA); Surfactant 10G from Fitzgerald Industries (Acton, MA, USA); 20× Borate, pH 8.5 and 10× PBST from Thermo Fisher Scientific (Waltham, MA, USA); PBS tablets from VWR (Radnor, PA, USA); BSA from Seracare Life Sciences (Milford, MA, USA).

Recombinant SARS-CoV-2 nucleocapsid analytes were purchased from Acro Biosystems (Cat. No. NUN-C5227), Creative Diagnostics (Cat. No. DAGC094), Genemedi (Cat. No. GMP-V-2019nCoV-N002), Genscript (Cat. No. Z03480-1), MyBiosource (Cat. No. MBS7135899), Sino Biological (Cat. No. 40588-V088), and The Native Analyte Co. (Cat. No. REC31812-100). Anti-SARS-CoV-2-nucleocapsid antibodies were sourced from many vendors; a complete list of antibodies screened in this work are provided in Table S1.

The following LFA materials were used for antibody screening: backed nitrocellulose (20 mm wide, CN95, Sartorius Lab Instruments GmbH & Co. KG, Otto-Brenner-Strafe 20, Göttingen, Germany), conjugate pad (10 mm wide, No. 6613, Ahlstrom-Munksjö, Oyj, Finland), sample pad (18 mm wide, Cat. No. 1281, Ahlstrom-Munksjö), wicking pad (14 mm wide, Cat. No. 440, Ahlstrom-Munksjö), cover tape (13 mm wide, Cat. No. 300H2, 3M, St. Paul, MN, USA) and backing card (50 mm wide, Cat. No. KN2211, Kenosha, Schweitzerlaan, The Netherlands).

All primers and probes, purified 2019-nCoV_N control plasmid, and Hs_RPP30 human control plasmid were purchased from IDT (Coralville, IA, USA). The Research Use Only (RUO) QIAamp Viral Mini Kit for RNA extraction was purchased from Qiagen (Hilden, Germany). The qScript XLT 1-Step RT-qPCR ToughMix was purchased from QuantaBio (Beverly, MA, USA). Molecular biology grade water was purchased from Fisher Scientific (Waltham, MA, USA).

A total of nine de-identified samples were purchased from Medix (Lombard, IL, USA). These samples included six SARS-CoV-2 positives and three negatives. All samples were de-identified and discarded after use and therefore did not require IRB approval.

RT-qPCR for detection of COVID-19 and quantification of SARS-CoV-2 viral load

The COVID-19 status of clinical samples used in this work was determined in-house using a multiplex RT-qPCR for the N1, N2, and RP targets.[9] Briefly, 70 or 140 µL of sample was purified using the QIAamp Viral Mini Kit according to the manufacturer's protocol[10] and purified RNA was eluted in either 70 or 140 µL based on CDC recommendations.[11] The multiplexed reaction was performed using the qScript master mix from QuantaBio with N1 and RP primers and probe concentrations of 500 nM and 250 nM (final) and N2 primers and probe concentrations of 2000 nM and 500 nM (final). The probes used were N1-FAM, N2-AlexaFluor594, and RP-Cy5. For each reaction, 5 µL of sample was added to 15 µL of amplification mix. Samples were classified as positive if both N1 and N2 targets were detected with Ct values below 40 cycles.[12] Viral load was determined using a standard curve for the N1 target generated

from purified 2019-nCoV_N control plasmid. The SARS-CoV-2 control plasmid from IDT was quantified in-house using the BioRad QX200 Digital Droplet PCR System.

Analyte selection using Octet

Antibody–analyte interactions were evaluated with an Octet RED96 biolayer interferometry instrument (Molecular Devices, Sartorius AG, Göttingen, Germany). All measurements were performed in 96-well microplates (Greiner Bio-one, Frickenhausen, Germany) at ambient temperature. Antibodies were loaded at 25 nM in 1× Kinetics Buffer for 120 seconds and captured using AMC tips for mouse antibodies, AHC tips for humanized recombinant antibodies, and Protein A tips for rabbit antibodies. Materials for the Octet were purchased from Molecular Devices. New sensors were used for every reaction and no tip regeneration was performed.

Typical immobilization levels were 1 ± 0.2 nm for monoclonal antibodies, and 2 nm for rabbit polyclonal antibodies. Following the load step, all sensors were equilibrated to baseline for 120 seconds in 1× Kinetics Buffer. An association step was performed for 300 seconds with analyte at 100 nM quantity, followed by 300 second dissociation into 1× Kinetics buffer.

Antibody/analyte evaluation by SDS-PAGE

Analytes were evaluated for purity and size using SDS-PAGE. Concentration was measured for all proteins using BCA assay (Thermo Pierce cat. 23225). Samples were premixed 1× NuPAGE LDS Sample Buffer (4×, Thermo Pierce cat. NP0007) and heated at 70^{o}C for 10 minutes. Gels with a 4–12% Bis-Tris gradient were used to achieve separation. Coomassie Imperial Protein Stain (Thermo Pierce cat. 24615) was used to visualize bands. Novex Sharp Pre-stained protein standard (Thermo Fisher scientific) was used as a molecular weight marker.

Latex bead conjugation

For both test and control line detection conjugates, 400 nm carboxylic blue latex beads (Cat. No. CAB400NM, Magsphere, Pasadena CA, USA) were washed three times with 0.1 M MES buffer, pH 6. Then, latex beads were activated using EDC/NHS coupling reagents at 0.15 and 10 mg/mL respectively for 30 minutes. Afterwards, the blue latex particles were conjugated in 1× PBS, pH 7.2 to various anti-nucleocapsid antibodies at a w/w ratio of 30:1 and 10:1 (bead:antibody) for test and control line antibodies, respectively, for three hours. Finally, latex conjugates were quenched using 0.1 M ethanolamine before being washed and blocked with 6% (w/v) casein, final concentration 1.2%, overnight. The latex conjugates were stored in buffer containing 50 mM borate and 1% casein, pH 8.5. The latex conjugates were quantified using the spectrophotometer by measuring absorbance at 660 nm and comparing to absorbance of unconjugated beads.

LFA reagent deposition

Capture antibodies at 1 mg/mL in 1× PBS, pH 7.4 and 2.5% (w/v) sucrose were striped (ZX1010, BioDot, Irvine, CA, USA) on nitrocellulose CN95 and dried at 25°C for 30 min. The control line was striped at 0.75 mg/mL donkey anti-chicken IgY (Cat. No. 703-005-155, Jackson ImmunoResearch, West Grove, PA, USA). For antibody screening, the nitrocellulose was unblocked. The test and control lines were located at 8 mm and 13 mm from the upstream edge of the nitrocellulose membrane.

The conjugate pad was dip-coated with two blocking solutions. First, 6613 conjugate pads were soaked in a 0.05% (w/v) Tween 20 in diH_2O solution for 15–20 seconds and dried at 40°C for 60 min. Pads were again soaked in 50 mM borate, pH 8.5; 0.25% (w/v) Triton X-100; 1% (w/v) Surfactant 10G; 1% (w/v) sucrose; and 6% (w/v) casein for another 15–20 seconds. The conjugate pad was dried for 60 min at 40°C before assembly.

LFA Assembly

Card assembly was performed on a clamshell laminator (Matrix 2210, Kinematic Automation, Sonora CA, USA). Pads were placed on the backing card in the following order: nitrocellulose, cover tape, conjugate pad, sample pad, wicking pad. Individual strips (3.3 mm wide) were cut with a Matrix 2360 sheet cutter (Kinematic Automation) and assembled in cassettes (proprietary design) using an assembly roller (YK725, Kinbio Tech Co., Shanghai, China).

Hamilton screening procedure

Antibody pairs were screened on an integrated robotic system[8] used previously to test antibody performance directly on nitrocellulose. In this system, the Hamilton STAR automated liquid handling robot (Hamilton Company, Reno, NV, USA), camera (IDS UI-1460SE-C-H detector with a Tamron M118FM16 lens), custom plate that held up to 96 LFAs, and custom control software developed in-house were combined to allow rapid screening of antibody pairs directly in LFA format. The robot used 8-channel pipetting for parallel application to LFAs and the camera for imaging. The custom control software applied 1 µL of conjugate mix (0.15% anti-nucleocapsid-antibody–latex-bead test line conjugate and 0.1% or 0.05% chicken-IgY-antibody–latex-bead control line conjugate in 50 mM borate, pH 8.5) to the conjugate pad of the LFA. After a 10-minute delay to let the conjugate mix dry, 75 µL of sample, nucleocapsid protein, or buffer (2.5% BSA in PBST or 2.5% BSA and 1% IGEPAL in 1× PBS) was added to the sample pad. Images were acquired 20 minutes after sample addition. For each antibody pair, for positive and negative samples, four technical replicates were run in rounds with rNP, and three technical replicates were run in the round with pooled clinical samples.

Screening rNPs on LFAs

We conducted four rounds of testing using rNP as the target analyte, followed by one round using pooled NP positive swab samples from donors. The first round used the best-available-at-the-time rNP analyte, sourced from GeneMedi (GMP-V-2019nCoV-N002), at 50 ng/mL. The second through fourth rounds used a higher-affinity rNP analyte, sourced from Acro Biosystems (NUN-C5227), at 50, 25, and 10 ng/mL, respectively. The third and fourth rounds eliminated antibody pairs that performed poorly in the previous round and added new pairs as antibodies became commercially available. In other words, antibody pair combinations varied round-by-round. A complete list of pairs from all rounds is in Table S2.

Screening clinical samples on LFAs

In-house RT-qPCR was performed on banked nasopharyngeal clinical samples to confirm infection status prior to LFA testing (Table 1).

When testing clinical samples on the benchtop, test and control line conjugates were hand spotted prior to sample application. Four Ab pair conditions, of various levels of performance with rNP, were used for clinical sample validation. The test line conjugate was diluted to a final concentration of 0.10%

and control line chicken IgY conjugate to 0.15% in 50 mM borate, pH 8.5. First, 1 µL of conjugate mixture was pipetted onto the conjugate pad and allowed to dry at ambient temperature for 10 minutes prior to application of the sample. All samples were diluted 1:25 in sample buffer containing 2.5% BSA and 1% IGEPAL CA-630 in 1x PBS. Samples were incubated on ice for 30 minutes prior to use. Second, 75 µL of each sample diluted in sample buffer was added to the conjugate pad and run at ambient conditions inside a biosafety cabinet for 20 minutes prior to being read in an LFA reader (Axxin, Fairfield, Australia).

Clinical samples were pooled to conduct screening in Round 5 (Table S1). A 1:100 titration was confirmed to produce visibly weak signal intensity at the test line and was therefore used as the positive control antibody pair SiB-MM08 / SiB-R004 (capture antibody / detection antibody). Aliquots of 1:100 clinical pooled samples were prepared and stored at -80°C until thawed for a single experimental use, then discarded.

Data analysis

Image analysis for the integrated robotic system was performed with a custom Python-based tool developed in-house.[8] This tool identified the test and control lines, measured nitrocellulose background intensity, and reported line strength as the height of the strip-width-averaged, background-subtracted, peak pixel intensity in the red image channel. Faulty LFAs were identified by weak control lines and removed as outliers, however outlier removal was rare, occurring in fewer than 2% of all LFAs tested.

Antibody pair rankings were determined by comparing mean test line strength from tests run with analyte-positive samples (signal, S) versus from tests run with analyte-negative samples (non-specific binding or noise, N). Two comparisons, or metrics, were used, signal divided by noise (S/N) and signal subtracted by noise (S−N). Both metrics were used to ensure the best pairs had both high positive control and low negative control signals.

Image analysis for LFAs run on the benchtop was performed using an LED-based LFA reader (Axxin). This reader reported test and control lines strengths on a different scale from our custom robot image analysis tool, but previous validation experiments indicate good correlation between the outputs of the two algorithms (data not shown).

Results and Discussion

We performed bio-layer interferometry on recombinant nucleocapsid proteins (rNP analytes) for the purpose of selecting the most “native-like” rNP analyte for early LFA antibody screening. We first used the estimated R_{max} of five different rNP analytes to quantify binding affinity against a random selection of 21 anti-nucleocapsid-protein (α-NP) antibodies from seven vendors (Rockland, Novus Biologicals, Sino Biological, Creative Diagnostics, Bioss, Fitzgerald, and MyBiosource). R_{max} as a metric was calculated based on the theoretical saturation of 100% of the bound antibody (ligand) with the rNP analyte. In practice, analyte binding sites are not completely occupied, so the measured saturation value is typically less than R_{max}. Moreover, because R_{max} is proportional to analyte size, we were also able to detect aggregation or multimer formation in solution. Theoretically, the closer—and more

predictable—values were to R_{max} the more likely the analyte was to interact with antibodies as expected.

Among the rNP analytes available at the beginning of screening, we selected the rNP analyte from Genemedi (GM-rNP) as the starting analyte because the average R_{max} for GM-rNP across 21 different α-NP antibodies was closest to its theoretical R_{max} (data not provided). We subsequently obtained an rNP analyte from Acro Biosystems (AB-rNP) and determined, using the available α-NP antibodies at that time and a similar kinetic analysis as above, that it produced higher-affinity antibody interactions (on aggregate) than GM-rNP. Additional discussion of the differences between the two rNP analyte sources can be found in the supplemental information. None of rNP analyte sources, however, allowed for testing the effects of the patient sample nasal matrix, so clinical SARS-CoV-2 patient nasopharyngeal swab samples stored in viral transport medium (VTM) were also sourced. Separate pools containing six high positives and six negatives (by qRT-PCR, Table 1) were diluted to create the additional analyte source.

Table 1 | Banked samples were used to compare performance of select anti-nucleocapsid antibody pairs in LFAs. In total, six RT-qPCR-confirmed SARS-CoV-2 positives, three SARS-CoV-2 negatives, and two potential coronavirus cross-reactive samples were screened.

Clinical Pool	Patient ID/Cat. No.	Vendor	Volume ratio of pooled sample	SARS-CoV-2 qPCR Results (pos v neg)	SARS-CoV-2 Viral Load (c/µL)	MSD NP sample mean concentration (pg/mL)
+	352-COP-0023-0	LabCorp	0.18	+	2.58E+05	5.76E+05
+	352-COP-0050-0	LabCorp	0.23	+	3.99E+05	3.07E+05
+	352-COP-0056-0	LabCorp	0.088	+	5.58E+05	4.80E+05
+	352-COP-0090-0	LabCorp	0.16	+	9.79E+05	2.05E+05
+	352-COP-0099-0	LabCorp	0.18	+	1.69E+04	1.19E+05
+	352-COP-0100-0	LabCorp	0.16	+	7.26E+05	6.82E+05
-	352-CON-1001-0	LabCorp	0.17	-	-	0.00E+00
-	352-CON-1003-0	LabCorp	0.17	-	-	0.00E+00
-	352-CON-1005-0	LabCorp	0.17	-	-	4.08E+00
-	352-CON-1011-0	LabCorp	0.17	-	-	0.00E+00
-	352-CON-1012-0	LabCorp	0.17	-	-	0.00E+00
-	352-CON-1084-0	LabCorp	0.17	-	-	0.00E+00

The robotic screening system automated the first screening round against GM-rNP at 50 ng/mL in the round's positive tests, and a buffer control in the round's negative tests (Round 1). Subsequently, the robotic screening system automated three more rounds against AB-rNP at concentrations of 50, 25 and 10 ng/mL in each round's positive tests, and a buffer control in each round's negative tests (Rounds 2, 3, and 4, respectively). We stepped down the concentration of the AB-rNP in three successive rounds because as vendors developed (and we sourced) new α-NP antibodies, better antibody pairs emerged and the average signal intensity in the LFA tests reached the non-linear region of the response curve. The number of unique antibody pairs screened in all rNP rounds were 106, 150, 144, and 288, respectively. At the conclusion of each round, we carried over at least the top 20 antibody pairs by signal (average test line signal from positive LFA tests for a given pair) minus noise (average test line signal from negative LFA tests using a pair), or "S−N," and signal divided by noise, or "S/N," given

available stocks. Due to the time-dependent commercial availability of the antibodies, we considered Rounds 2 and 3 to be "weed-out" rounds and summarized their results in Figure S1. We subsequently considered Round 4 as a representative screen of the best-available-at-the-time antibodies against AB-rNP, in preference to Rounds 2 and 3.

After four rounds against the two rNP analytes, the robotic screening system automated a final round of screening against diluted, pooled, positive patient samples in the round's positive tests, and diluted, pooled, negative patient samples in the round's negative tests (Round 5). This last round screened the 26 antibodies which had not been previously dropped due to poor performance and for which we had sufficient stock (676 pairs). The purpose of this final screen was two-fold: (1) determine if relative performance of top pairs from rounds against the rNP analytes persisted in a round against clinical samples, and (2) we had the opportunity to compare, head-to-head, the relative performance of all α-NP antibody pairs. The only antibody pairs excluded from this round performed poorly in several prior rounds (rankings for all pairs in all rounds in Table S2). Additionally, three newly available antibodies were screened in the clinical pool round for the first time. Antibody pairs containing these antibodies performed well, appearing as a top-five pair twice (pair indices 736 and 608,Table S2) and nine times in the top 20 (pair indices 736, 608, 686, 30, 689, 708, 815, 416, and 171, Table S2). The five best antibody pairs against the diluted clinical sample pool (Round 5) are listed in Table 2 along with the top five pairs against GM-rNP (Round 1) and against the lowest-concentration of AB-rNP (Round 4). The top antibody pairs against the three different analyte sources are highlighted in the scatter plots (S−N vs. S/N) in Figure 1, and in the average of S−N and S/N rankings in Table S3.

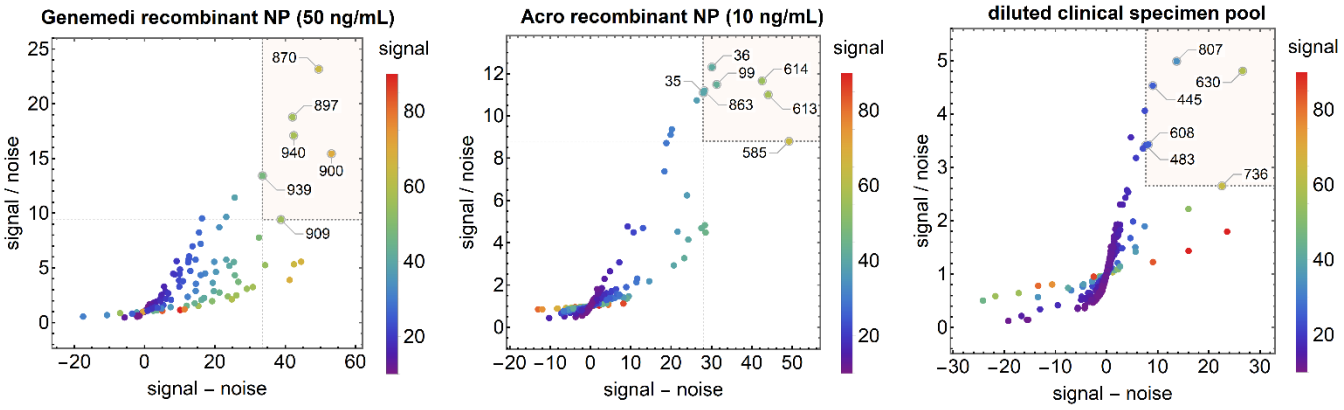

Figure 1 | Performance of 1021 individual antibody pairs as a function of signal / noise and signal − noise. The pairs in the top 10 for both metrics are shown in the highlighted box.

Nine of the top-20 antibody pairs screened against GM-rNP and 15 of the top-20 pairs screened against the lowest concentration of AB-rNP were available to be screened against the diluted clinical sample pool. Of these 24 antibody pairs, few performed well in the screen against the diluted clinical sample pool. One of these 24 (pair index 900, Table S2) had an average rank (i.e. average of S−N rank and S/N rank) of 24.5 in the clinical sample screen, whereas the average rank of the other 23 pairs ranged from 110 to 671.5, with a median value of 336.5 (where the total number of pairs in this round was 676).

This disagreement highlighted the importance of using native analyte in realistic sample types when screening antibody pairs for assay development. We were unable to completely determine in the course of this work whether performance against GM-rNP or AB-rNP better predicted performance against the diluted clinical sample pool (although neither appeared to predict the latter results as noted above) because every round consisted of a slightly different set of antibodies (as antibodies became commercially available or became depleted from vendor stocks). Surrogate samples can provide the advantages of more reliable sourcing, more experimental control, and less expense than clinical samples. However, it can be difficult to create surrogate samples that are completely representative of real samples, not least due to patient-to-patient variability in the matrix. Additionally, we sourced clinical samples that were stored in VTM, which would not be the diluent used in a clinical LFA test. Nonetheless, we chose to move to the clinical samples at first availability, and to test the best-to-date antibodies still available against a diluted sample pool, to get as close to real samples as possible.

Table 2 | Antibody pairs in the top 20 for both S/N and S−N are ranked according to the round in which they were tested. Table S2 contains a complete list of all pairs that were screened.

			Average rank		
Index	**Capture antibody**	**Detection antibody**	**Genemedi rNP**	**Acro rNP**	**Sample pool**
Top 5 performers against Genemedi recombinant NP (rNP) at 50 ng/mL					
870	Sino Biological 40143-MM08	Creative Diagnostics DCABH-4693	**1.5**	-	573
900	Sino Biological 40143-MM08	Sino Biological 40143-R004	**2.5**	-	28
897	Sino Biological 40143-MM08	Sino Biological 40143-MM05	**4**	12.5	328.5
940	Sino Biological 40143-R001	Sino Biological 40143-MM08	**4**	16	87
939	Sino Biological 40143-R001	Sino Biological 40143-MM05	**7.5**	13.5	-
Top 5 performers against Acro recombinant NP (rNP) at 10 ng/mL					
614	Genemedi GMP-V-2019nCoV-Nab001	Sino Biological 40143-MM08	-	**2.5**	491
36	Bioss bsm-41411M	Sino Biological 40143-MM08	-	**3**	309
99	Bioss bsm-41413M	Sino Biological 40143-MM08	-	**3.5**	400.5
613	Genemedi GMP-V-2019nCoV-Nab001	Sino Biological 40143-MM05	-	**4**	221.5
585	Genemedi GMP-V-2019nCoV-Nab001	Creative Diagnostics CABT-CS037	-	**5.5**	671.5
Top 5 performers against diluted clinical sample pool					
630	Genemedi GMP-V-2019nCoV-Nab002	Genemedi GMP-V-2019nCoV-Nab001	-	-	**1.5**
807	MyBiosource MBS569961	Fitzgerald 10-2853	-	-	**3.5**
445	Fitzgerald 10-2854	MyBiosource MBS569939	-	-	**5.5**
736	MyBiosource MBS569937	Leinco LT7000	-	-	**6.5**
608	Genemedi GMP-V-2019nCoV-Nab001	Meridian Life Science 9548	-	-	**7.5**

While performance (by S−N or S/N) was not necessarily consistent across sample type, one important outcome of running a large antibody screen in an LFA format was the identification of pairs that non-specifically bind at the test line. Non-specific binding is a major problem for LFA tests, as they represent false positive results in real-world applications. Screening data from non-LFA formats sometimes does not predict non-specific binding in an LFA format, because of the unique interplay of flow dynamics and chemical kinetics across reagents and materials in an LFA. We have found that

screening data from the high-throughput robotic platform does predict non-specific binding in the LFA even when screened with different sample matrices, such as clinical negatives at multiple dilutions (Figure S3). Additionally, several rounds of negative sample screening data can often be combined—even if positive samples are varied across rounds—if the negative samples are consistent across rounds, as was the case here. Combined negative sample data was used to remove pairs from contention when non-specific binding was greater than a chosen threshold (e.g., a nominal specificity target), which was helpful because the number of candidate pairs was large. This method reduced the likelihood that a high positive signal was primarily driven by non-specific binding (a false positive), which would incorrectly suggest that a candidate antibody pair deserved further optimization.

Conclusions

We screened 1021 α-NP antibody pairs against three sources of SARS-CoV-2 nucleocapsid protein, and identified multiple pairs, inclusive of antibodies from several different commercially available sources, as promising candidates towards the development of lateral flow assays for the detection of SARS-CoV-2. Further work is required for the development of a point-of-care test for SARS-CoV-2, though the high-performance antibodies identified in this work may hasten its development. The antibody pairs identified as top-ranking pairs against pooled clinical samples should be interpreted as worth further testing, not necessarily a precisely ordered list of the best candidate reagents for developing an LFA. The top-ranking pairs against clinical samples have demonstrated strong affinity for (some form of) native antigen in the context of lateral flow through nitrocellulose. However, we suggest that multiple of these top antibody pairs be tested further by anyone attempting to develop an LFA using these data, as the precise interaction of all assay components, materials, and methods (especially when different from the conditions in our tests) can affect pair performance.

Acknowledgements

Funding provided by The Global Good Fund and Global Health Labs, a nonprofit organization created by Gates Ventures and the Gates Foundation to develop innovative solutions to address unmet needs in primary health care centers and the last mile.

References

(1) Zhu, N.; Zhang, D.; Wang, W.; Li, X.; Yang, B.; Song, J.; Zhao, X.; Huang, B.; Shi, W.; Lu, R.; Niu, P.; Zhan, F.; Ma, X.; Wang, D.; Xu, W.; Wu, G.; Gao, G. F.; Tan, W. A Novel Coronavirus from Patients with Pneumonia in China, 2019. *N. Engl. J. Med.* 2020, *382* (8), 727–733. https://doi.org/10.1056/NEJMoa2001017.

(2) Coronavirus disease (COVID-19) Situation Report https://www.who.int/docs/default-source/coronaviruse/situation-reports/20200723-covid-19-sitrep-185.pdf?sfvrsn=9395b7bf_2 (accessed Jul 23, 2020).

(3) Larremore, D. B.; Wilder, B.; Lester, E.; Shehata, S.; Burke, J. M.; Hay, J. A.; Tambe, M.; Mina, M. J.; Parker, R. Test Sensitivity Is Secondary to Frequency and Turnaround Time for COVID-19 Surveillance. *medRxiv* 2020, 2020.06.22.20136309. https://doi.org/10.1101/2020.06.22.20136309.

(4) He, X.; Lau, E. H. Y.; Wu, P.; Deng, X.; Wang, J.; Hao, X.; Lau, Y. C.; Wong, J. Y.; Guan, Y.; Tan, X.; Mo, X.; Chen, Y.; Liao, B.; Chen, W.; Hu, F.; Zhang, Q.; Zhong, M.; Wu, Y.; Zhao, L.; Zhang, F.; Cowling, B. J.; Li, F.; Leung, G. M. Temporal Dynamics in Viral Shedding and Transmissibility of COVID-19. *Nat. Med.* 2020, *26* (5), 672–675. https://doi.org/10.1038/s41591-020-0869-5.

(5) Alexandersen, S.; Chamings, A.; Bhatta, T. R. SARS-CoV-2 Genomic and Subgenomic RNAs in Diagnostic Samples Are Not an Indicator of Active Replication. *medRxiv* 2020, 2020.06.01.20119750. https://doi.org/10.1101/2020.06.01.20119750.

(6) Expression of interest - FIND https://www.finddx.org/eoi-covid19-ag-rdt/ (accessed Jul 23, 2020).

(7) COVID-19 Target product profiles for priority diagnostics to support response to the COVID-19 pandemic v.0.1 https://www.who.int/publications/m/item/covid-19-target-product-profiles-for-priority-diagnostics-to-support-response-to-the-covid-19-pandemic-v.0.1 (accessed Aug 8, 2020).

(8) Huynh, T.; Cate, D. M.; Nichols, K. P.; Weigl, B. H.; Anderson, C. E.; Gasperino, D. J.; Harston, S. P.; Hsieh, H. V.; Marzan, R.; Williford, J. R.; Oncina, C. I.; Glukhova, V. A. Integrated Robotic System for the Development Lateral Flow Assays. In *2019 IEEE Global Humanitarian Technology Conference, GHTC 2019*; Institute of Electrical and Electronics Engineers Inc., 2019. https://doi.org/10.1109/GHTC46095.2019.9033066.

(9) Byrnes, S. A.; Gallagher, R.; Steadman, A.; Bennett, C.; Rivera, R.; Ortega, C.; Motley, S. T.; Jain, P.; Weigl, B. H.; Connelly, J. T. Multiplexed and Extraction-Free Amplification for Simplified SARS-CoV-2 RT-PCR Tests. *medRxiv* 2020, 2020.05.21.20106195. https://doi.org/10.1101/2020.05.21.20106195.

(10) QIAamp Viral RNA Mini Handbook - QIAGEN https://www.qiagen.com/us/resources/resourcedetail?id=c80685c0-4103-49ea-aa72-8989420e3018&lang=en (accessed Jul 23, 2020).

(11) *CDC 2019-Novel Coronavirus (2019-NCoV) Real-Time RT-PCR Diagnostic Panel For Emergency Use Only Instructions for Use*.

(12) Bustin, S. A.; Benes, V.; Garson, J. A.; Hellemans, J.; Huggett, J.; Kubista, M.; Mueller, R.; Nolan, T.; Pfaffl, M. W.; Shipley, G. L.; Vandesompele, J.; Wittwer, C. T. The MIQE Guidelines: Minimum Information for Publication of Quantitative Real-Time PCR Experiments. *Clin. Chem.* 2009, *55* (4), 611–622. https://doi.org/10.1373/clinchem.2008.112797.